Journal of Biomechanics 46 (2013) 2053–2059

Contents lists available at SciVerse ScienceDirect

Journal of Biomechanics

journal homepage: www.elsevier.com/locate/jbiomech
www.JBiomech.com

Relationship between shear elastic modulus and passive muscle force: An ex-vivo study

Terry K. Koo [a,*], Jing-Yi Guo [a], Jeffrey H. Cohen [b], Kevin J. Parker [c]

[a] Department of Research, New York Chiropractic College, Seneca Falls, NY, United States
[b] Nimmo® Educational Foundation, Pittsburgh, PA, United States
[c] Department of Electrical & Computer Engineering, University of Rochester, Rochester, NY, United States

ARTICLE INFO

Article history:
Accepted 21 May 2013

Keywords:
Shear wave elastography
Passive muscle force
Reliability

ABSTRACT

As muscle is stretched, it reacts with increasing passive resistance. This passive force component is important for normal muscle function. Unfortunately, direct measurement of passive muscle force is still beyond the current state-of-the-art. This study aimed to investigate the feasibility of using Supersonic shear wave elastography (SSWE) to indirectly measure passive muscle force. Sixteen gastronomies pars externus and 16 tibialis anterior muscles were dissected from 10 fresh roaster chickens. For each muscle specimen, the proximal bone–tendon junction was kept intact with its tibia or femur clamped in a fixture. Calibration weights (0–400 g in 25 g per increment) were applied to the distal tendon via a pulley system and muscle elasticity was measured simultaneously using SSWE. The measurements were repeated for 3 cycles. The elasticity-load relationship of each tested muscle for each loading cycle was analyzed by fitting a least-squares regression line to the data. Test-retest reliability was evaluated using intraclass correlation coefficient (ICC). Results demonstrated that the relationships between SSWE elasticity and passive muscle force were highly linear for all the tested muscles with coefficients of determination ranging between 0.971 and 0.999. ICCs were 0.996 and 0.985, respectively, for the slope and y-intercept parameters of the regression lines, indicating excellent reliability. These findings indicate that SSWE, when carefully applied, can be a highly reliable technique for muscle elasticity measurements. The linear relationship between SSWE elasticity and passive muscle force identified in the present study demonstrated that SSWE may be used as an indirect measure of passive muscle force.

1. Introduction

As a skeletal muscle is being stretched, it reacts with increasing passive resistance. This passive force is important to normal muscle function (Gajdosik, 2001). In human experiments, dynamometers have been widely used to measure passive torques at different joint angles (McNair et al., 2002; Nordez et al., 2009; Weiss et al., 1986), but these measures are the resultant of several synergistic muscles, ligaments, and articular structures surrounding the joint, not to mention the confounding effects of estimating the moment arms of various structures on passive muscle force calculation. Hence, they are non-specific measures of individual muscle forces. Direct, non-invasive, in-vivo measurement of muscle force is still beyond the current state-of-the-art.

In the past two decades, researchers have been exploring different techniques to indirectly measure muscle forces. Some zinvestigators used indentation devices and utilized either linear (Zheng and Mak, 1999) or non-linear elastic (Koo et al., 2011) models to estimate lumped elasticity parameters of all the tissue layers (i.e. skin, fascia, fat, and muscle) underneath the indenter. Again, these are non-specific measures of muscle. It is also not known how the lumped transverse elasticity measured by these indentation devices correlates with passive muscle force. Others measured intramuscular pressure and assumed that it could provide an indirect measurement of muscle force (Baumann et al., 1979; Sejersted and Hargens, 1995; Crenshaw et al., 1995; Ballard et al., 1998). However, direct measurements of intramuscular pressure and passive muscle force in isolated rabbit tibialis anterior muscle only revealed a modest correlation with wide variation between specimens (Davis et al., 2003), indicating that intramuscular pressure may not be a reliable indirect measure of passive muscle force. Some researchers used different elastography techniques, including vibration elastography imaging (Levinson et al., 1995; Parker and Lerner, 1992; Yamakoshi et al., 1990), compression elastography (Ophir et al., 1991, 1999), magnetic resonance elastography (Bensamoun et al., 2007; Dresner et al., 2001), transient shear wave elastography (Gennisson et al., 2003, 2005), acoustic radiation force imaging

* Correspondence to: Foot Levelers Biomechanics Research Laboratory, New York Chiropractic College, 2360 State Route 89, Seneca Falls, NY 13148, United States. Tel.: +1 315 568 3158; fax: +1 315 568 3204.
E-mail address: tkoo@nycc.edu (T.K. Koo).

0021-9290/$ - see front matter © 2013 Elsevier Ltd. All rights reserved.
http://dx.doi.org/10.1016/j.jbiomech.2013.05.016

(Nightingale et al., 2002), crawling wave imaging (Wu et al., 2004, 2006), and Supersonic Shear Wave Elastography (Gennisson et al., 2010; Lacourpaille et al., 2012) etc., to estimate localized muscle elasticity by assessing the response of the muscle to applied perturbation of various kinds. Although understanding the physiological meaning of muscle elasticity is essential in clinical diagnosis and research on musculoskeletal injuries and movement-related disorders, and the application of this knowledge to patient care is central to rehabilitation, studies attempting to explore the relationships between muscle elasticity and muscle force are rare (Bouillard et al., 2011, 2012; Dresner et al., 2001; Levinson et al., 1995; Maisetti et al., 2012; Nordez et al., 2008; Nordez and Hug, 2010).

Supersonic Shear wave Elastography (SSWE) is the current state-of-the-art ultrasound technology that uses acoustic radiation force induced by ultrasound beams to perturb underlying tissues (Bercoff et al., 2004b). This force induces shear waves which propagate within the tissue. By focusing the push forces at different depths in tissues at high speed, shear waves are coherently summed; this substantially increases the propagation distance (Bercoff et al., 2004a). As the shear waves propagate, they are captured by the ultrasound transducer at a frame rate up to 20,000 Hz. Shear wave propagation speed (V) is then estimated at each pixel. Shear elastic modulus (G) can then be directly deduced by the following equation (Bercoff et al., 2004b):

$$G = \rho V^2 \tag{1}$$

where ρ is the muscle density which is assumed to be 1000 kg/m^3.

SSWE can provide quantitative elasticity maps in real time with color scale expressed in kilopascals, and SSWE does not require external compression and/or vibration. Hence, it should be less skill-dependent as compared with other elastography modalities. The objectives of the current study were to: (1) evaluate the accuracy and test-retest reliability of SSWE; (2) validate the feasibility of using SSWE to indirectly measure passive muscle force; and (3) explore the effects of architectural parameters on elastic properties of passive muscles. This knowledge will allow us to better understand the physiological meaning of elasticity in passive muscles.

2. Methods

2.1. Phantom experiment

The accuracy of SSWE to measure quantitative values of elasticity was evaluated using an elasticity QA phantom (Model 049, CIRS, Norfolk, VA). The phantom consisted of 4 spherical inclusions at 15 mm deep with different elasticity values embedded within the background material. Five elasticity measurements were made for each spherical inclusion as well as the background material and their ensemble means were calculated and compared with those specified by the manufacturer.

2.2. Ex-vivo chicken experiment

2.2.1. Muscle Specimens

Sixteen gastrocnemius pars externus (GE) and 16 tibialis anterior (TA) muscles were dissected from 10 fresh roaster chickens with mean weight ($\pm$SD) of 3.56 kg ($\pm$0.34 kg). Among 7 of them, both the left and right TA and GE muscles were dissected and tested. The GE is a unipennate muscle, whereas the TA is a fusiform muscle. Before the passive loading experiment, each muscle specimen was allowed to reach room temperature and sprayed regularly with isotonic saline solution to avoid dehydration. The proximal bone–tendon junction was kept intact with its tibia (for TA) or femur (for GE) clamped in a fixture. Calibration weights were applied to the distal tendon via a cable and pulley system (Fig. 1). This setup allowed the muscle to be placed under various amount of passive tension. After the passive loading experiment, each muscle specimen was removed from the bone and its mass (m) and length (l_m) were measured by a triple beam balance scale (Fisher Scientific, Model 711-T) and a digital caliper respectively. Muscle length was defined as the distance between the proximal and distal muscle-tendon junction at its slack length. Cross sectional area (CSA) was then estimated as follows:

$$CSA = m/\rho l_m \tag{2}$$

where ρ is muscle density which is assumed to be 1000 kg/m^3.

Since the chicken TA has two heads, one attached to the distal femur and the other to the proximal tibia (Pautou et al., 1982), and our passive loading experiment was conducted with only the tibia being fixed, it is reasonable to assume that all passive force was transmitted through the tibial head during the passive loading experiment. Hence, the mass and length of the TA muscles reported in this study were those of the tibial head only.

2.2.2. Experimental setup

An Aixplorer ultrasound scanner (Supersonic Imagine, France), coupled with a 50 mm, 14–5 MHz linear ultrasound transducer was set to SSWE mode with "musculoskeletal" preset to measure shear elastic modulus of the muscle specimens. A multi-articulated arm (Manfrotto, Italy) was used to position and hold the transducer so that the same measurement site could be imaged at the same orientation throughout the passive loading experiment. The transducer was placed perpendicular to the muscle belly of each dissected muscle along its longitudinal axis (Fig. 1). A generous amount of ultrasound gel was applied on the surface of the muscle belly. A small gel-filled gap between the transducer and the muscle surfaces was maintained by adjusting a linear actuator (Zaber Technologies, Vancouver, Canada) so that the effects of compression on elasticity measurement were minimized.

Prior to the commencement of the passive loading experiment, we acquired an elastography image sample and reviewed its corresponding shear wave propagation movie to confirm that the specimen and transducer were properly setup. Briefly speaking, shear wave propagation movie is a special tool within the research software provided by the manufacturer. It allows for direct visualization of the propagation of the shear waves induced by acoustic radiation forces. Ideally, the acoustic radiation forces induce a pair of strong plane shear waves that propagate

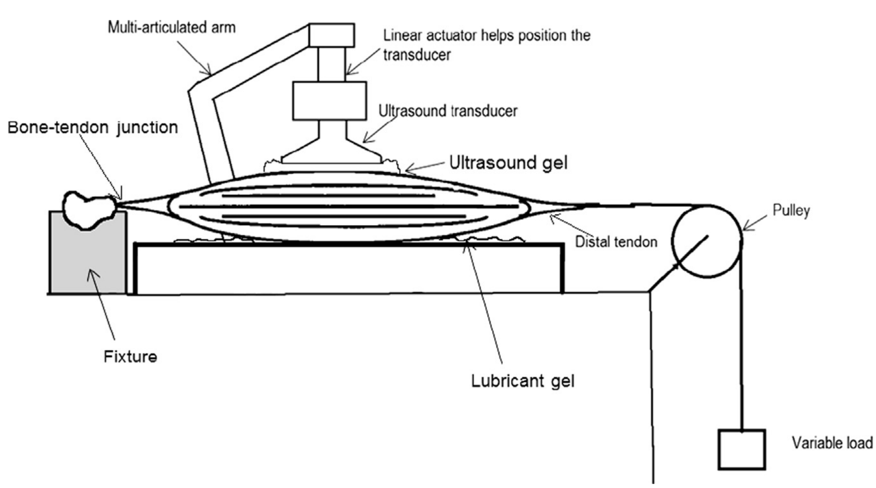

Fig. 1. A schematic diagram of the experimental setup. The transducer was placed on the muscle belly of each dissected muscle along its longitudinal axis. Passive muscle tension was applied to the distal tendon of muscle through a pulley system. Lubricant gel was applied on the table surface to reduce friction when the muscle was being elongated.

in opposite directions (Fig. 2A). The stiffer the medium, the faster the shear wave will move. With strong shear waves, the shear wave propagation speed can be reliably estimated at each pixel from the shear wave propagation movie using cross correlation algorithms. Conversely, if the induced shear waves are weak, as they propagate, dissipation will occur rapidly and hence, shear wave signals will disperse quickly (Fig. 2B), making the shear wave propagation speed estimation unreliable. Therefore, by observing the integrity of the shear wave propagation, we can assess the quality of our elasticity measurements. The setup process was repeated if the quality of the shear wave propagation was unsatisfactory.

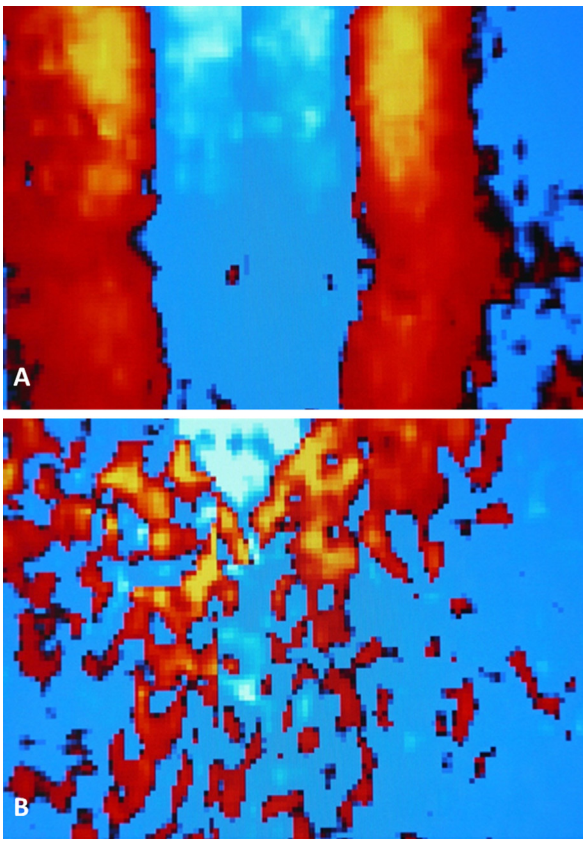

Fig. 2. Examples of (A) good and (B) poor shear wave propagation images. Each image represents a snapshot from a corresponding shear wave propagation movie. They were obtained by photo-taking a snapshot from the shear wave propagation movie displayed in the monitor of the Aixplorer system. The shear wave propagation can be affected by many factors such as transducer placement with respect to muscle fiber direction, the amount of ultrasound gel between transducer and tissue interfaces, the depth of the tissue to be imaged, the thickness of skin and subcutaneous tissue, etc.

2.2.3. *Elasticity measurements*

For each tested muscle, a square-shape elastography window was positioned at a location that approximated its maximum thickness as observed in the B-mode image. The size of the elastography window was set to cover the whole muscular area while avoiding the upper and lower borders of the tested muscle (Fig. 3). A circular region was centered within the elastography window at its maximum diameter and the average shear elastic modulus over the circular region was calculated by the Aixplorer software (Fig. 3). The average diameters of the circular regions were 9.8 ± 0.79 mm and 10.1 ± 0.65 mm for the TA and GE, respectively.

After the muscle specimen and the transducer were properly setup, the passive load was stepwise increased from 0 to 400 g in 25 g per increment or until the mean shear elastic modulus of the muscle specimen got beyond ~80 kPa, whichever came first. Limiting the imposed elastic modulus safeguarded the muscle specimens from permanent damage. At each load, after the passive load was applied, the elastography window was first allowed to stabilize for 5 s before the 1st elastography image was acquired. The 2nd and 3rd elastography images were then captured 3 and 6 s later. For each image, the average shear elastic modulus within the circular region was measured and the ensemble mean among the 3 images was regarded as the shear elastic modulus of the tested muscle at that load. The loading cycle was repeated three times with the 1st cycle regarded as pre-conditioning (Fig. 4). Throughout the experiment, the elastography window was fixed at the same location (Fig. 3) so that the elasticity data measured at different cycles and loads could be directly compared.

2.2.4. *Data analysis*

Passive elasticity-load relationship of each tested muscle for each loading cycle was analyzed by fitting a least-squares regression line to the data:

$$G = sT + G_o \quad (3)$$

Herein, G represents the shear elastic modulus of the muscle due to the passive tension (T) generated by the calibration weights; s represents the rate of increase in shear elastic modulus per unit load; and G_o represents the shear elastic modulus of the muscle at its slack length. Coefficient of determination (R^2), s, and $G_o$of each regression line were computed. Test-retest reliability of (1) SSWE elasticity and (2) the curve fitting parameters (i.e. s and G_o) were evaluated based on the data of the 2nd and 3rd cycles using a single-rating, absolute agreement, 2-way mixed model (i.e. intraclass correlation coefficient $[ICC]_{3,1}$). Two-way repeated measures ANOVAs were performed to test the effects of (1) side (i.e. left and right), and (2) muscle (i.e. GE and TA) on each dependent variable (i.e. G_o, s, CSA, l_m, and m). A confidence level of 0.05 was chosen for all statistical tests.

3. Results

Results of elasticity QA phantom experiment are shown in Table 1. The absolute differences from the reference values were 0.4, 0.2, 0.3, 0.9, 0.3 kPa respectively for the type 1, type 2, type 3, type 4, and the background material and the coefficients of variation were 1.9%, 0.6%, 1.3%, 4.3%, and 0.3% respectively, indicating excellent accuracy and repeatability of the SSWE elasticity measurements.

Our data revealed a linear relationship between SSWE elasticity and passive muscle force for all the 32 tested muscles (Fig. 4).

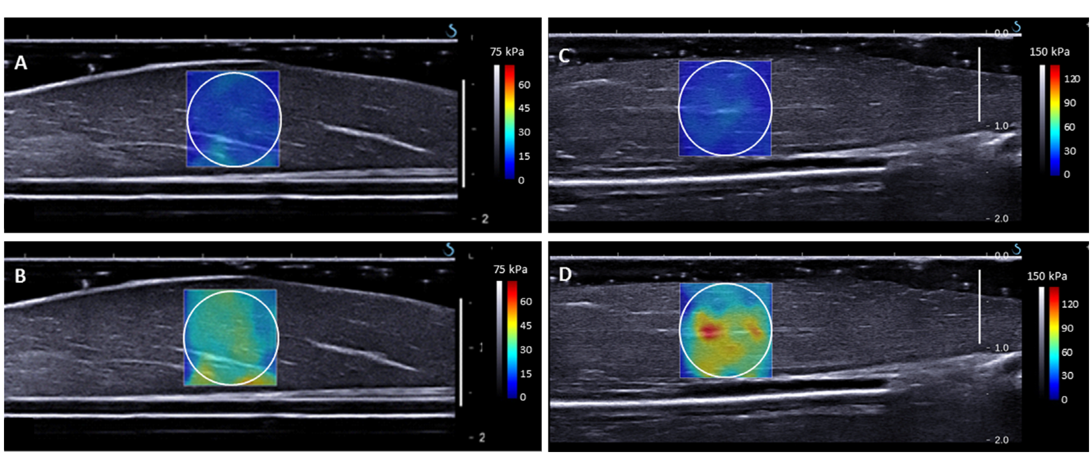

Fig. 3. Examples of elastography images of gastrocnemius pars externus (GE) and tibialis anterior (TA). (A) GE at 25 g; (B) GE at 350 g; (C) TA at 25 g; (D) TA at 200 g. Mean shear elastic modulus (G) was measured over the circular region. As revealed in these images, GE is a unipennate muscle, whereas TA is a fusiform muscle.

Mean (± SD) coefficient of determination (R^2) equaled 0.988 (± 0.005) with the range between 0.974 and 0.994.

Test-retest reliability of SSWE elasticity measurement was excellent with ICC equaled 0.995. The linear regression lines of different loading cycles were also very similar with the ICCs of s and G_o equaling 0.996 and 0.985, respectively.

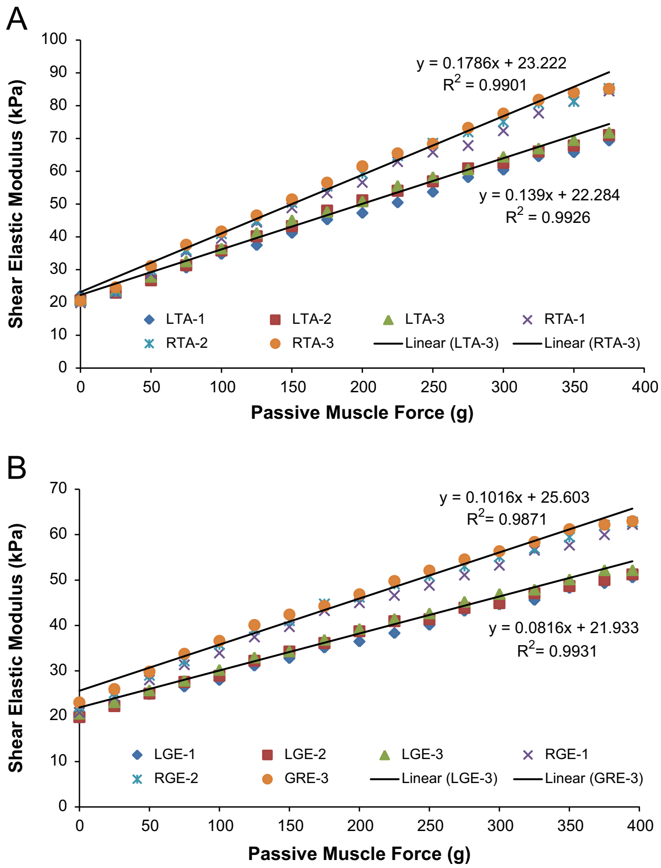

Fig. 4. Typical example of elasticity-load plot of (A) tibialis anterior and (B) gastrocnemius pars externus muscles. Salient findings include: (1) elasticity-load data of the 1st loading cycle was slightly different but they were very similar between the 2nd and 3rd cycles, and hence, the 1st cycle was regarded as pre-conditioning; and (2) a highly linear relationship was noted between elasticity and passive muscle force. LTA-n: left tibialis anterior, cycle n; RTA-n: right tibialis anterior, cycle n; LGE-n: left gastrocnemius pars externus, cycle n; RGE-n: right gastrocnemius pars externus, cycle n; Linear (LTA-3): linear regression line for LTA-3; Linear (RTA-3): linear regression line for RTA-3; Linear (LGE-3): linear regression line for LGE-3; Linear (RGE-3): linear regression line for RGE-3; and R^2: coefficient of determination.

Mean (± SD) of mass (m), cross sectional area (CSA), length, rate of increase in shear elastic modulus per unit load (s), and shear elastic modulus at slack length (G_o) of the tested muscles are summarized in Table 2. Two-way repeated measures ANOVA revealed that except G_o (p=0.879), all other dependent variables (i.e. m, CSA, l_m and s) were significantly different between the TA and GE muscles (m: $p < 0.0001$; CSA: $p < 0.0001$; l_m p=0.016; s: $p < 0.0001$). More specifically, m and CSA of the GE were significantly larger than the TA; l_m of the TA was significantly longer than the GE; and s of the TA was significantly larger than that of the GE. However, there were no significant main effects of side on each dependent variable (G_o: p=0.243; s: p=0.793; CSA: p=0.476; l_m: p=0.285; m: p=0.887). There was also no interaction effect (i.e. muscle x side) for each dependent variable (G_o: p=0.352; s: p=0.629; CSA: p=0.969; l_m: p=0.749; m: p=0.566).

s vs. the reciprocal of cross sectional area (1/CSA) and the reciprocal of muscle mass (1/m), respectively, were plotted in Fig. 5A and B. Similarly, G_o vs. 1/CSA and 1/m respectively, were plotted in Fig. 6A and 6B.

4. Discussion

Data of the present study shows that with proper setup, SSWE is an accurate, reliable, and repeatable technology to measure elasticity. According to the manufacturer recommendations (Aixplorer User Guide, 2011), for optimal measurement results, it is imperative to avoid manual compression and hold the transducer steadily during SSWE measurements. These requirements are readily achievable by utilizing a mounting apparatus like the one described in the present study. Indeed, our high repeatability can be attributed to our success of: (1) maintaining the same transducer orientation and location throughout the experiment; (2) maintaining a small gel-filled gap between the transducer and muscle/phantom surfaces; and (3) confirming the validity of the elasticity measurements based on the quality of shear wave signals.

Few investigators have attempted to understand the relationship between muscle elasticity and passive muscle force (Dresner et al., 2001; Maisetti et al., 2012; Nordez et al., 2008). Nordez et al. (2008) used transient elastography to measure shear elastic modulus of human gastrocnemius muscle and reported a fairly strong linear relationship (mean R^2=0.812)

Table 1
Accuracy of the SSWE elasticity measurements.

	Type 1	Type 2	Type 3	Type 4	Background
Reference shear elastic modulus (kPa)	2.7 ± 1.0	4.7 ± 1.3	15.0 ± 2.7	26.7 ± 4.0	8.3 ± 2.0
Shear elastic modulus measured by SSWE (kPa)	3.1 ± 0.06	4.5 ± 0.03	14.7 ± 0.2	25.8 ± 1.1	8.6 ± 0.02
Coefficients of variation (%)	1.9	0.6	1.3	4.3	0.3

Table 2
Mean (± SD) of mass (m), cross sectional area (CSA), length (l_m), rate of increase in shear elastic modulus per unit load (s), and shear elastic modulus at slack length (G_o) of the tested muscles.

Muscle	Side	m (g)	CSA (mm^2)	l_m (mm)	s (kPa/g)	G_o (kPa)
Tibialis anterior (TA)	Left	12.8 ± 0.64	126.9 ± 5.8	101.3 ± 5.6	0.163 ± 0.044	25.3 ± 2.2
	Right	13.1 ± 0.83	129.6 ± 4.0	100.4 ± 5.4	0.170 ± 0.031	23.7 ± 6.3
Gastrocnemius pars externus (GE)	Left	21.7 ± 1.45	233.4 ± 8.1	92.9 ± 4.1	0.080 ± 0.012	25.8 ± 5.9
	Right	21.5 ± 1.45	235.8 ± 14.3	91.2 ± 4.3	0.079 ± 0.019	22.5 ± 5.0

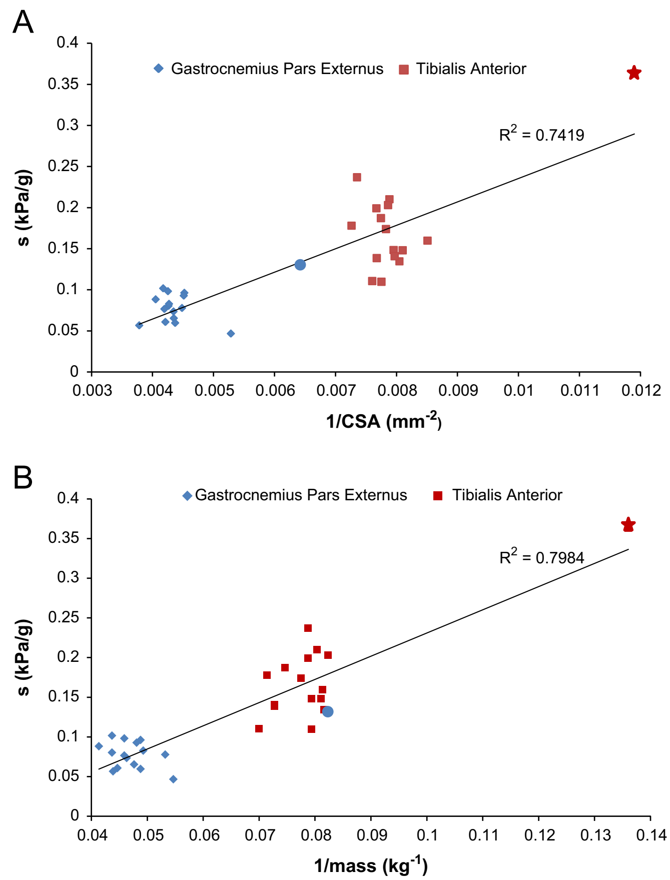

Fig. 5. Relationships between rate of increase in shear elastic modulus per unit load (s) and architectural parameters. (A) s vs. the reciprocal of cross sectional area ($1/CSA$) and (B) s vs. the reciprocal of muscle mass ($1/m$). Please note that the specific data points TA (★) and GE (●) were dissected from a chicken with substantially smaller mass and CSA. R^2 stands for coefficient of determination.

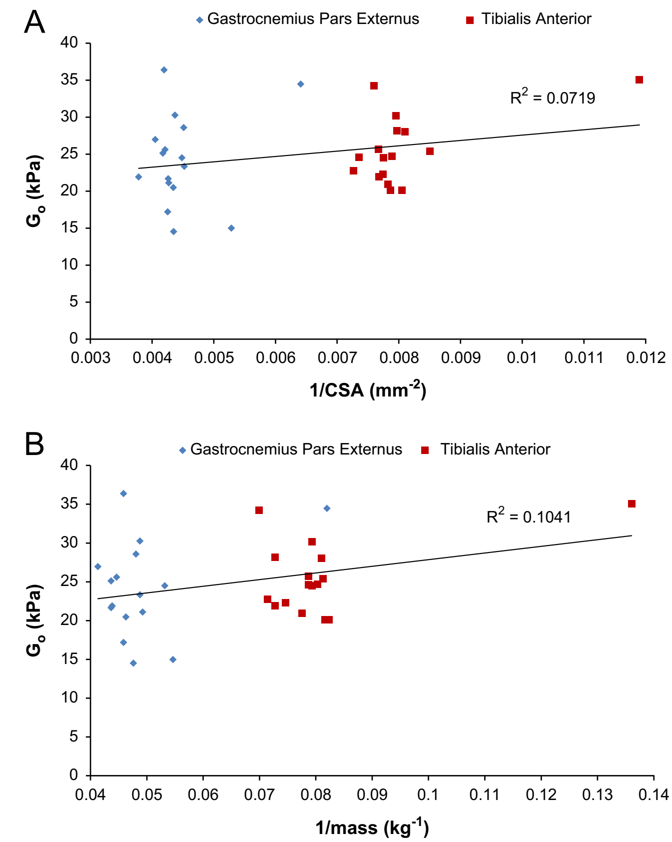

Fig. 6. (A) Relationships between shear elastic modulus of the muscle at its slack length (G_o) and muscle architectural parameters. (A) G_o vs. the reciprocal of cross sectional area ($1/CSA$) and (B) G_o vs. the reciprocal of muscle mass ($1/m$). R^2 stands for coefficient of determination.

between shear elastic modulus and passive ankle torque. Given that joint torque is the resultant of multiple structures and each structure has a different moment arm, it is hard to directly infer a linear relationship between passive muscle tension and shear elastic modulus from their study. Maisetti et al. (2012) conducted a human subject experiment on gastrocnemius muscle and provided the first evidence to support the idea that SSWE elasticity may provide an indirect estimation of passive muscle force. However, the passive muscle forces reported by Maisetti were not measured directly but predicted by a musculoskeletal model with many empirical assumptions (Hoang et al., 2005; Nordez et al., 2010). The present ex-vivo chicken muscle study provided further evidence to support Maisetti's claim. Our results demonstrated that there is a strong linear relationship (mean $R^2 = 0.988$; range: 0.974 and 0.994) between SSWE elasticity and passive muscle tension in all 32 dissected muscles, and hence, we are confident that SSWE elasticity measurements can be an indirect measure of passive muscle force. To the author's knowledge, this is the first study that directly correlates passive muscle force with shear elastic modulus measured by SSWE. Similar linear increases in shear elastic modulus with passive tension have also been observed in a MRE study of ex-vivo bovine muscles (Dresner et al., 2001). In addition, when comparing our coefficient of determination values with those of intramuscular pressure measurements (Davis et al., 2003), it appears that SSWE (R^2 range: 0.974–0.994) is superior to intramuscular pressure (R^2 range: 0.672–0.982) for indirect measurement of passive muscle force.

Dresner et al. (2001) proposed a model to explain the linear relationship between passive muscle tension (T) and elasticity (G_p):

$$G_p = \frac{kT}{CSA} + G_o \tag{4}$$

where k is a proportionality factor to reflect the partial storage of energy, CSA is the cross sectional area of the muscle, and G_o represents the elasticity of a relaxed muscle at its slack length. Based on this model, if k is a constant, s in Eq. (3) should be proportional to the reciprocal of muscle cross sectional area. Even though CSAs of the tested muscles in the present study were mainly clustered in two regions, we were still able to get a fairly good linear fit to the data ($R^2 = 0.742$) (Fig. 5A). These results appear to support Dresner's model. Interestingly, the fit between s and the reciprocal of muscle mass was even better ($R^2 = 0.798$) (Fig. 5B). This may be attributed to the measurement errors of the muscle lengths. The scattering appearance of these plots may also reflect the fact that k is not a constant among muscles.

There were significant differences between TA and GE muscles in terms of their architectural parameters (i.e. l_m, m, and CSA). This architectural difference appears to explain the difference in s (i.e. the rate of increase in shear elastic modulus per unit load) between the TA and GE muscles (Fig. 5). However, when comparing G_o (shear elastic modulus of the muscle at its slack length) between TA and GE muscles, no significant difference was found. In addition, when G_o was plotted against the reciprocal of muscle mass and the reciprocal of muscle CSA, the coefficients of determination (R^2) were very small (Fig. 6). These imply that muscle architecture should have no significant effect on G_o. Instead, we noted that G_o could vary widely from muscle to muscle (Fig. 6). This may be related to the difference in the amount and type of collagen fibers between muscles (Kovanen et al., 1984).

Utilizing sonoelastography, Levinson et al. (1995) found that valid muscle elasticity measurements can only be achieved parallel to the muscle fibers. We observed similar phenomena in SSWE. If SSWE measurements were acquired in the transverse direction, poor shear wave signals were observed, which implies that elasticity measurements in the transverse direction are questionable. It appears that the complicated boundary conditions were a significant factor for propagation perpendicular to the muscle fibers. In addition, in an anisotropic media such as muscle, the shear wave velocity depends on direction with respect to fiber orientation, so this must be carefully controlled. Hence, to acquire valid SSWE elasticity data, it is imperative to position the transducer parallel to the muscle fibers. Appropriate transducer alignment can be achieved when several fascicles can be traced without interruption across the B-mode image (Blazevich et al., 2006).

The present study was not without limitation. First, we only confirmed the accuracy of SSWE measurements up to 26.7 kPa using a commercially available elasticity QA phantom. This range is rather small compared to the measurement range reported in our ex-vivo animal experiment. It is uncertain whether SSWE measurements are accurate for higher shear elastic modulus values. Future studies should confirm this by custom-making an elasticity QA phantom with higher elasticity range. Second, it is an ex-vivo animal study. It is unknown whether the results can be directly extended to live human subjects. Unless an intraoperative experiment similar to the present study can be conducted in patients undergoing tendon transfer surgery, there is no way to directly correlate passive muscle force and SSWE elasticity in human subjects. Hence, the use of an ex-vivo animal model in the present study is justified. Nonetheless, owing to our consistent findings among all 32 muscles and the supported evidence from the literature (Dresner et al., 2001; Maisetti et al., 2012; Nordez et al., 2008), we are confident that our findings can be extended to human subjects. Perhaps a human cadaveric study may provide further evidence to support this claim. Third, except for one chicken, all the chickens we picked were similar in weights. This resulted in a clustering effect of our CSA and mass data in Fig. 5. To better analyze the relationships between stiffening rate (s), CSA, and muscle mass, muscles with a wide spread of CSA and mass should be picked. Forth, we have to admit that our muscle length measurements were rather empirical. That may affect our CSA calculation. More sophisticated methods should be employed to normalize the measured muscle length based on laser diffraction based sarcomere length measurement (Lieber et al., 1984; Murray et al., 2000). Fifth, for a non-fusiform muscle like GE, the change of pennation angle induced by stretching may affect the SSWE measurement. Nonetheless, as revealed in Figs. 3A and B, the pennation angles of GE did not change substantially within our testing range, indicating that it should have no major effect on the accuracy of our SSWE measurements.

The force generated by skeletal muscles is the summation of active and passive components. The passive force originates from stretching the extracellular connective tissues (Cavagna, 1977; Heerkens et al., 1987) and titan protein (Labeit and Kolmerer, 1995; Wang et al., 1993), and the active force is produced by the cross-bridging of actin and myosin contractile proteins. Hence, they are from different origins. The present study revealed a highly linear relationship between passive muscle force and SSWE elasticity. Recent work also revealed a linear relationship between (1) SSWE elasticity and active muscle force (Deffieux et al., 2008; Bouillard et al., 2011) as well as (2) SSWE elasticity and EMG amplitude (Nordez and Hug, 2010). Thus, SSWE elasticity appears to be a promising technique to indirectly measure individual muscle forces. Future studies should be devoted to understanding the relative stiffening effects of passive and active forces on SSWE elasticity of the same muscle.

5. Conclusion

SSWE, when carefully applied, can be a highly accurate and reliable technique for muscle elasticity measurements. The linear relationship between SSWE elasticity and passive muscle force identified in the present study demonstrated that SSWE elasticity may be used as an indirect measure of passive muscle force.

Conflict of interest statement

The authors confirm that there is no conflict of interest in this manuscript.

Acknowledgments

The authors would like to thank Anatomy Department of New York Chiropractic College for providing dissection facilities. This study was supported by Nimmo® Educational Foundation.

References

Aixplorer User Guide. SuperSonic Imagine S.A. 2011.
Ballard, R.E., Watenpaugh, D.E., Breit, G.A., Murthy, G., Holley, D.C., Hargens, A.R., 1998. Leg intramuscular pressures during locomotion in humans. Journal of Applied Physiology 84, 1976–1981.
Baumann, J.U., Sutherland, D.H., Hanggi, A., 1979. Intramuscular pressure during walking: an experimental study using the wick catheter technique. Clinics in Orthopaedics and Related Research 145, 292–299.
Bensamoun, S.F., Ringleb, S.I., Chen, Q., Ehman, R.L., An, K.N., Brennan, M., 2007. Thigh muscle stiffness assessed with magnetic resonance elastography in hyperthyroid patients before and after medical treatment. Journal of Magnetic Resonance Imaging 26 (3), 708–713.
Bercoff, J., Tanter, M., Fink, M., 2004a. Sonic boom in soft materials: the elastic Cerenkov effect. Applied Physics Letters 84 (12), 2202–2204.
Bercoff, J., Tanter, M., Fink, M., 2004b. Supersonic shear imaging: a new technique for soft tissue elasticity mapping. IEEE Transactions on Ultrasonics, Ferroelectrics, and Frequency Control 51 (4), 396–409.
Blazevich, A.J., Gill, N.D., Zhou, S., 2006. Intra- and intermuscular variation in human quadriceps femoris architecture assessed in vivo. Journal of Anatomy 209 (3), 289–310.
Bouillard, K., Nordez, A., Hug, F., 2011. Estimation of individual muscle force using elastography. PLoS One 6 (12), e29261.
Bouillard, K., Hug, F., Guevel, A., Nordez, A., 2012. Shear elastic modulus can be used to estimate an index of individual muscle force during a submaximal isometric fatiguing contraction. Journal of Applied Physiology 113, 1353–1361.
Cavagna, G.A., 1977. Storage and utilization of elastic energy in skeletal muscle. Exercise and Sport Sciences Reviews 5, 89–129.
Crenshaw, A.G., Karlsson, S., Styf, J., Backlund, T., Friden, J., 1995. Knee extension torque and intramuscular pressure of the vastus lateralis muscle during eccentric and concentric activities. European Journal of Applied Physiology and Occupational Physiology 70, 13–19.
Davis, J., Kaufman, K.R., Lieber, R.L., 2003. Correlation between active and passive isometric force and intramuscular pressure in the isolated rabbit tibialis anterior muscle. Journal of Biomechanics 36, 505–512.
Deffieux, T., Gennisson, J.L., Tanter, M., Fink, M., 2008. Assessment of the mechanical properties of the musculoskeletal system using 2-D and 3-D very high frame rate ultrasound. IEEE Transactions on Ultrasonics, Ferroelectrics, and Frequency Control 55, 2177–2190.
Dresner, M.A., Rose, G.H., Rossman, P.J., Muthupillai, R., Manduca, A., Ehman, R.L., 2001. Magnetic resonance elastography of skeletal muscle. Journal of Magnetic Resonance Imaging 13 (2), 269–276.
Gajdosik, R.L., 2001. Passive extensibility of skeletal muscle: review of the literature with clinical implications. Clinical Biomechanics 16 (2), 87–101.
Gennisson, J.L., Catheline, S., Chaffai, S., Fink, M., 2003. Transient elastography in anisotropic medium: application to the measurement of slow and fast shear wave speeds in muscles. The Journal of the Acoustical Society of America 114 (1), 536–541.
Gennisson, J.L., Cornu, C., Catheline, S., Fink, M., Portero, P., 2005. Human muscle hardness assessment during incremental isometric contraction using transient elastography. Journal of Biomechanics 38 (7), 1543–1550.

Gennisson, J.L., Deffieux, T., Mace, E., Montaldo, G., Fink, M., Tanter, M., 2010. Viscoelastic and anisotropic mechanical properties of in vivo muscle tissue assessed by supersonic shear imaging. Ultrasound in Medicine & Biology 36 (5), 789–801.

Heerkens, Y.F., Woittiez, R.D., Kiela, J., Huijing, P.A., Huson, A., van Ingen Schenau, G. J., Rozendal, R.H., 1987. Mechanical properties of passive rat muscle during sinusoidal stretching. Pflugers Archiv: European Journal of Physiology 409 (4–5), 438–447.

Hoang, P.D., Gorman, R.B., Todd, G., Gandevia, S.C., Herbert, R.D., 2005. A new method for measuring passive length-tension properties of human gastrocnemius muscle in vivo. Journal of Biomechanics 38 (6), 1333–1341.

Koo, T.K., Cohen, J.H., Zheng, Y., 2011. A mechano-acoustic indentor system for in vivo measurement of nonlinear elastic properties of soft tissue. Journal of Manipulative and Physiological Therapeutics 34 (9), 584–593.

Kovanen, V., Suominen, H., Heikkinen, E., 1984. Mechanical properties of fast and slow skeletal muscle with special reference to collagen and endurance training. Journal of Biomechanics 17, 725–735.

Labeit, S., Kolmerer, B., 1995. Titins: giant proteins in charge of muscle ultrastructure and elasticity. Science 270 (5234), 293–296.

Lacourpaille, L., Hug, F., Bouillard, K., Hogrel, J.Y., Nordez, A., 2012. Supersonic shear imaging provides a reliable measurement of resting muscle shear elastic modulus. Physiological measurement 33 (3), N19–28.

Levinson, S.F., Shinagawa, M., Sato, T., 1995. Sonoelastic determination of human skeletal muscle elasticity. Journal of Biomechanics 28 (10), 1145–1154.

Lieber, R.L., Yeh, Y., Baskin, R.J., 1984. Sarcomere length determination using laser diffraction. Effect of beam and fiber diameter. Biophysical Journal 45 (5), 1007–1016.

Maisetti, O., Hug, F., Bouillard, K., Nordez, A., 2012. Characterization of passive elastic properties of the human medial gastrocnemius muscle belly using supersonic shear imaging. Journal of Biomechanics 45 (6), 978–984.

McNair, P.J., Hewson, D.J., Dombroski, E., Stanley, S.N., 2002. Stiffness and passive peak force changes at the ankle joint: the effect of different joint angular velocities. Clinical Biomechanics 17 (7), 536–540.

Murray, W.M., Buchanan, T.S., Delp, S.L., 2000. The isometric functional capacity of muscles that cross the elbow. Journal of Biomechanics 33 (8), 943–952.

Nightingale, K., Nightingale, R., Stutz, D., Trahey, G., 2002. Acoustic radiation force impulse imaging of in vivo vastus medialis muscle under varying isometric load. Ultrasonic Imaging 24 (2), 100–108.

Nordez, A., Casari, P., Mariot, J.P., Cornu, C., 2009. Modeling of the passive mechanical properties of the musculo-articular complex: acute effects of cyclic and static stretching. Journal of Biomechanics 42 (6), 767–773.

Nordez, A., Foure, A., Dombroski, E.W., Mariot, J.P., Cornu, C., McNair, P.J., 2010. Improvements to Hoang et al.'s method for measuring passive length-tension properties of human gastrocnemius muscle in vivo. Journal of Biomechanics 43 (2), 379–382.

Nordez, A., Gennisson, J.L., Casari, P., Catheline, S., Cornu, C., 2008. Characterization of muscle belly elastic properties during passive stretching using transient elastography. Journal of Biomechanics 41 (10), 2305–2311.

Nordez, A., Hug, F., 2010. Muscle shear elastic modulus measured using supersonic shear imaging is highly related to muscle activity level. Journal of Applied Physiology 108 (5), 1389–1394.

Ophir, J., Alam, S.K., Garra, B., Kallel, F., Konofagou, E., Krouskop, T., Varghese, T., 1999. Elastography: ultrasonic estimation and imaging of the elastic properties of tissues. Proceedings of the Institution of Mechanical Engineers. Part H, Journal of Engineering in Medicine 213 (3), 203–233.

Ophir, J., Cespedes, I., Ponnekanti, H., Yazdi, Y., Li, X., 1991. Elastography: a quantitative method for imaging the elasticity of biological tissues. Ultrasonic imaging 13 (2), 111–134.

Parker, K.J., Lerner, R.M., 1992. Sonoelasticity of organs: shear waves ring a bell. Journal of Ultrasound in Medicine 11 (8), 387–392.

Pautou, M.P., Hedayat, I., Kieny, M., 1982. The pattern of muscle development in the chick leg. Archives of Anatomy, Microscopy and Experimental Morphology 71 (4), 193–206.

Sejersted, O.M., Hargens, A.R., 1995. Intramuscular pressures for monitoring different tasks and muscle conditions. Advances in Experimental Medicine and Biology 384, 339–350.

Wang, K., McCarter, R., Wright, J., Beverly, J., Ramirez-Mitchell, R., 1993. Viscoelasticity of the sarcomere matrix of skeletal muscles. The titin-myosin composite filament is a dual-stage molecular spring. Biophysical Journal 64 (4), 1161–1177.

Weiss, P.L., Kearney, R.E., Hunter, I.W., 1986. Position dependence of ankle joint dynamics—I. Passive mechanics. Journal of Biomechanics 19 (9), 727–735.

Wu, Z., Hoyt, K., Rubens, D.J., Parker, K.J., 2006. Sonoelastographic imaging of interference patterns for estimation of shear velocity distribution in biomaterials. The Journal of the Acoustical Society of America 120 (1), 535–545.

Wu, Z., Taylor, L.S., Rubens, D.J., Parker, K.J., 2004. Sonoelastographic imaging of interference patterns for estimation of the shear velocity of homogeneous biomaterials. Physics in Medicine and Biology 49 (6), 911–922.

Yamakoshi, Y., Sato, J., Sato, T., 1990. Ultrasonic imaging of internal vibration of soft tissue under forced vibration. IEEE Transactions on Ultrasonics, Ferroelectrics, and Frequency Control 37 (2), 45–53.

Zheng, Y., Mak, A.F., 1999. Effective elastic properties for lower limb soft tissues from manual indentation experiment. IEEE Transactions on Rehabilitation Engineering 7 (3), 257–267.